Self-energy and lifetime of Shockley and image states on Cu(100) and Cu(111): Beyond the GW approximation of many-body theory

M. G. Vergniory[1,2], J. M. Pitarke[1,3], and P. M. Echenique[2,4]

[1]*Materia Kondentsatuaren Fisika Saila, UPV/EHU, and Unidad Física Materiales CSIC-UPV/EHU,*
644 Posta kutxatila, E-48080 Bilbo, Basque Country, Spain
[2]*Donostia International Physics Center (DIPC),*
Manuel de Lardizabal Pasealekua, E-20018 Donostia, Basque Country, Spain
[3]*CIC nanoGUNE Consolider, Mikeletegi Pasealekua 56, E-2009 Donostia, Basque Country, Spain*
[4]*Materialen Fisika Saila, UPV/EHU, and Unidad Física Materiales CSIC-UPV/EHU,*
1071 Posta kutxatila, E-20018 Donostia, Basque Country, Spain
(Dated: February 2, 2008)

We report many-body calculations of the self-energy and lifetime of Shockley and image states on the (100) and (111) surfaces of Cu that go beyond the GW approximation of many-body theory. The self-energy is computed in the framework of the $GW\Gamma$ approximation by including short-range exchange-correlation (XC) effects both in the screened interaction W (beyond the random-phase approximation) and in the expansion of the self-energy in terms of W (beyond the GW approximation). Exchange-correlation effects are described within time-dependent density-functional theory from the knowledge of an adiabatic *nonlocal* XC kernel that goes beyond the local-density approximation.

I. INTRODUCTION

At metal surfaces there exist specific electronic states not present in the bulk, which can be classified as intrinsic (crystal-induced) surface states[1] and image-potential (Rydberg-like) states.[2,3] Intrinsic surface states are originated by the symmetry breaking at the surface, they have their maximum near the surface, and they are classified as Tamm[4] and Shockley[5] states; in particular, intrinsic Shockley surface states typically occur in the gap of free-electron-like s,p bands near the Fermi level.[6,7] Image-potential states appear as a result of the self-interaction that an electron near the surface suffers from the polarization charge it induces at the surface, and they occur in the vacuum region of metal surfaces with a band gap near the vacuum level.[8]

Figure 1 illustrates Shockley and image-potential states in the gap of the ΓL projected band structure of the (100) and (111) surfaces of Cu. If an electron or hole is added to the solid at one of these states, inelastic coupling of the excited quasiparticle with the crystal, which can be experimentally observed through a variety of spectroscopies,[9,10,11,12,13,14] may occur through electron-electron (e-e) and electron-phonon (e-ph) scattering. The decay rate due to the e-ph interaction, which is relatively important only in the case of excited Shockley holes near the Fermi level, has been investigated recently by using the Eliashberg function.[15] Accurate many-body calculations of the decay rate due to the e-e interaction were first carried out for image states on the (100) and (111) surfaces of Cu.[16,17] Since then, many-body calculations of the e-e decay have been reported for a variety of simple, noble and transition metals.[18,19,20,21] Nevertheless, existing calculations have been typically performed within the G^0W^0 approximation of many-body theory,[22,23,24,25] with no inclusion of exchange and correlation (XC) ef-

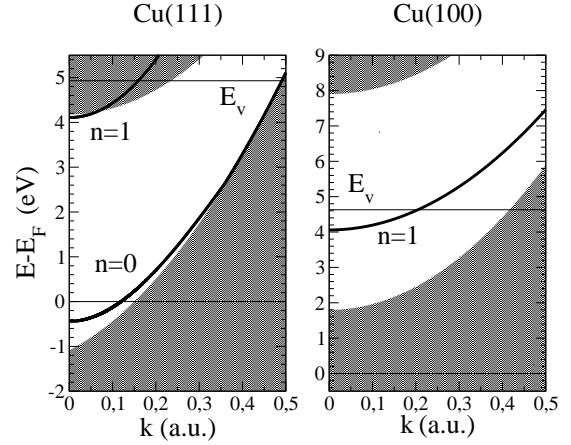

FIG. 1: The ΓL projected bulk band structure (shaded areas) of the (111) and (100) surfaces of Cu. The solid lines represent Shockley ($n = 0$) and image-potential ($n = 1$) surface-state bands.

fects. Exceptions are (i) a calculation of the e-e decay rate of image states on the (100) and (111) surfaces of Cu that incorporates XC effects in an adiabatic local-density approximation (ALDA)[17] and (ii) an approximate evaluation of the lifetime of Shockley states in the noble metals that incorporates the exchange contribution to the self-energy.[20]

In this paper, we report extensive calculations of the screened interaction, the self-energy, and the e-e inelastic lifetime of Shockley and image states on the (100) and (111) surfaces of Cu that go beyond the G^0W^0 approximation. Short-range XC effects are incorporated both in the description of the dynamical screening of the many-electron system [we go beyond the random-phase approximation (RPA) in the evaluation of the screened interaction W] and in the expansion of the electron self-

energy in terms of W [we go beyond the GW approximation]. This is the $GW\Gamma$ approximation of many-body theory,[26,27] which treats on the same footing XC effects between pairs of electrons within the Fermi sea (screening electrons) and between the excited electron and the Fermi sea.

Mahan and Sernelius[26] showed that the inclusion, within the $GW\Gamma$ approximation, of the same vertex function in the screened interaction and the numerator of the self-energy yields results for the band-width of a homogeneous electron gas very similar to those obtained in the G^0W^0 approximation, due to a large cancellation of vertex corrections. Large cancellations were also observed to occur in the decay rates of image[17] and bulk[28] states in the noble metals, by incorporating XC effects in the ALDA. In the decay of low-energy bulk states below the vacuum level energy transfers $\hbar\omega$ are well below the Fermi energy and momentum transfers $\hbar q$ are typically smaller than $2\hbar q_F$, q_F being the magnitude of the Fermi wave vector, so that one can safely assume that both q and ω are small and XC effects can, therefore, be incorporated in the ALDA. However, in the case of Shockley and image states the ALDA might lead to spurious results, due to the presence of small local values of the Fermi wave vector in a region where the electron density is small. Hence, here we use an adiabatic *nonlocal* XC kernel that accurately describes XC effects in the limit of a homogeneous electron gas of arbitrary density and which has been succesful in the description of the XC contribution to the jellium surface energy.[29]

It has been argued in the past that a realistic first-principles description of the electronic band structure is of key importance in the determination of the inelastic lifetime of bulk electronic states in the noble metals.[30] The main conclusion drawn in Ref. 30 was that in the case of the noble metals deviations from electron dynamics in a free gas of sp electrons mainly originate in the participation of d electrons in the screening of electron-electron interactions. The role of occupied d bands in the dynamics of excited surface-state electrons and holes on silver surfaces was later investigated via a polarizable medium giving rise to additional screening,[31] and it was concluded that d electrons do not participate significantly in the screening of the interaction between surface states (which are located near the surface) and the Fermi gas of the solid.[32]

In order to investigate the dynamics of Shockley and image states on Cu surfaces, we assume that the density of valence electrons in the solid varies only along the z axis, which is taken to be normal to the surface. Hence, our calculations start by solving the single-particle time-independent Schrödinger equation of electrons moving in a physically motivated one-dimensional (1D) model potential that is known to correcly reproduce the behaviour of sp valence states and accurately describes, in particular, the projected bulk band gap and the binding energy of the Shockley and the first image state.[33] The eigenfunctions and eigenvalues of such an effective single-particle hamiltonian are then used to compute the screened interaction, the $GW\Gamma$ self-energy, and the e-e decay rates of Shockley and image states. For comparison, we also compute G^0W^0, G^0W, and $GW^0\Gamma$ decay rates, with no inclusion of XC effects, with inclusion of XC effects beyond the RPA in the screened interaction W alone, and with inclusion of XC effects beyond the G^0W^0 in the expansion of the electron self-energy in terms of the RPA screened interaction W^0, respectively. Our results indicate that (i) although the use of the ALDA leads to spurious results for the screened interaction, a more realistic adiabatic *nonlocal* description of XC effects yields inelastic lifetimes of Shockley and image states that esentially coincide with those obtained in the ALDA, and (ii) the overall effect of short-range XC is small and $GW\Gamma$ linewidths are close to their G^0W^0 counterparts, as occurs in the case of low-energy bulk states.[28]

The paper is organized as follows. Explicit expressions for the e-e decay rate of surface-state electrons and holes at solid surfaces are derived in Sec. II, in the $GW\Gamma$ approximation of many-body theory. The results of numerical calculations of the screened interaction, the self-energy, and the decay rate of Shockley and image states on the (100) and (111) surfaces of Cu are presented in Sec. III. The summary and conclusions are given in Sec. IV. Unless stated otherwise, atomic units (a.u.) are used throughout, i.e., $e^2 = \hbar = m_e = 1$.

II. THEORY

Let us consider an arbitrary many-electron system of density $n_0(\mathbf{r})$. In the framework of many-body theory, the decay rate (or reciprocal lifetime) of a quasiparticle (electron or hole) that has been added in the single-particle state $\phi_i(\mathbf{r})$ of energy ε_i is obtained as the projection of the imaginary part of the self-energy $\Sigma(\mathbf{r}, \mathbf{r}'; \varepsilon_i)$ over the quasiparticle-state itself[24]

$$\tau_i^{-1} = \mp 2 \int d\mathbf{r} \int d\mathbf{r}' \phi_i^*(\mathbf{r}) \mathrm{Im}\Sigma(\mathbf{r}, \mathbf{r}'; \varepsilon_i) \phi_i(\mathbf{r}'), \qquad (1)$$

where the $\mp$ sign in front of the integral should be taken to be minus or plus depending on whether the quasiparticle is an electron ($\varepsilon_i \geq \varepsilon_F$) or a hole ($\varepsilon_i \leq \varepsilon_F$), respectively, ε_F being the Fermi energy.

To lowest order in a series-expansion of the self-energy in terms of the frequency-dependent screened interaction $W(\mathbf{r}, \mathbf{r}'; \omega)$, the self-energy is obtained by integrating the product of the interacting Green function $G(\mathbf{r}, \mathbf{r}'; \varepsilon_i - \omega)$ and the screened interaction $W(\mathbf{r}, \mathbf{r}'; \omega)$, and is therefore called the GW self-energy. If one further replaces the interacting Green function by its noninteracting counterpart $G^0(\mathbf{r}, \mathbf{r}'; \varepsilon_i - \omega)$, one finds the G^0W self-energy and from Eq. (1) the following expression for the G^0W reciprocal lifetime:

$$\tau_i^{-1} = \mp 2 \sum_f \int d\mathbf{r} \int d\mathbf{r}' \phi_i^*(\mathbf{r}) \phi_f^*(\mathbf{r}')$$

$$\times \ \mathrm{Im}\, W(\mathbf{r}, \mathbf{r}'; |\varepsilon_i - \varepsilon_f|)\, \phi_i(\mathbf{r}')\, \phi_f(\mathbf{r}), \qquad (2)$$

where the sum is extended over a complete set of single-particle states $\phi_f(\mathbf{r})$ of energy ε_f ($\varepsilon_F \le \varepsilon_f \le \varepsilon_i$ or $\varepsilon_i \le \varepsilon_f \le \varepsilon_F$). Equation (2) exactly coincides with the result one would obtain from the lowest-order probability per unit time for an excited electron or hole in an initial state $\phi_i(\mathbf{r})$ of energy ε_i to be scattered into the state $\phi_f(\mathbf{r})$ of energy ε_f by exciting a Fermi system of interacting electrons from its many-particle ground state to some many-particle excited state.[34]

The interaction $W(\mathbf{r}, \mathbf{r}'; \omega)$ entering Eq. (2) can be rigurously expressed as follows

$$W(\mathbf{r}, \mathbf{r}'; \omega) \ = \ v(\mathbf{r}, \mathbf{r}') + \int d\mathbf{r}_1 \int d\mathbf{r}_2\, v(\mathbf{r}, \mathbf{r}_1)$$
$$\times \ \chi(\mathbf{r}_1, \mathbf{r}_2; \omega)\, v(\mathbf{r}_2, \mathbf{r}'), \qquad (3)$$

$v(\mathbf{r}, \mathbf{r}')$ representing the bare Coulomb interaction and $\chi(\mathbf{r}, \mathbf{r}'; \omega)$ being the time-ordered density-response function of the many-electron system, which for the positive frequencies ($\omega > 0$) entering Eq. (2) coincides with the retarded density-response function of linear-response theory. In the framework of time-dependent density-functional theory (TDDFT),[35] the *exact* retarded density-response function is obtained by solving the following integral equation:[36]

$$\chi(\mathbf{r}, \mathbf{r}'; \omega) = \chi^0(\mathbf{r}, \mathbf{r}'; \omega) + \int d\mathbf{r}_1 \int d\mathbf{r}_2\, \chi^0(\mathbf{r}, \mathbf{r}_1; \omega)$$
$$\times \{ v(\mathbf{r}_1, \mathbf{r}_2) + f^{xc}[n_0](\mathbf{r}_1, \mathbf{r}_2; \omega) \}\, \chi(\mathbf{r}_2, \mathbf{r}'; \omega), \qquad (4)$$

where $\chi^0(\mathbf{r}, \mathbf{r}'; \omega)$ denotes the density-response function of noninteracting Kohn-Sham electrons, i.e., independent electrons moving in the effective Kohn-Sham potential of density-functional theory (DFT). The frequency-dependent XC kernel $f^{xc}[n_0](\mathbf{r}, \mathbf{r}'\omega)$ is the functional derivative of the frequency-dependent XC potential $V_{xc}[n](\mathbf{r}, \omega)$ of TDDFT, to be evaluated at $n_0(\mathbf{r})$. In the RPA, $f^{xc}[n_0](\mathbf{r}, \mathbf{r}'; \omega)$ is set equal to zero and Eq. (2) yields the so-called G^0W^0 (or G^0W-RPA) reciprocal lifetime.

The xc kernel $f^{xc}[n_0](\mathbf{r}, \mathbf{r}'; \omega)$, which is absent in the RPA, accounts for the presence of an XC hole associated to all screening electrons in the Fermi sea. Hence, one might be tempted to conclude that the full G^0W approximation [with the formally exact screened interaction W of Eq. (3)] should be a better approximation than its G^0W^0 counterpart [with the screened interaction W evaluated in the RPA]. However, the XC hole associated to the excited hot electron is still absent in the G^0W approximation. Therefore, if one goes beyond RPA in the description of W, one should also go beyond the G^0W approximation in the expansion of the electron self-energy in powers of W. By including XC effects both beyond RPA in the description of W and beyond G^0W in the description of the self-energy,[26,27] the so-called $GW\Gamma$ approximation yields a lifetime broadening that is of the

G^0W form [see Eq. (2)], but with the actual screened interaction $W(\mathbf{r}, \mathbf{r}'; \omega)$ of Eq. (3) replaced by a new effective screened interaction

$$\tilde{W}(\mathbf{r}, \mathbf{r}'; \omega) = v(\mathbf{r}, \mathbf{r}') + \int d\mathbf{r}_1 \int d\mathbf{r}_2\, \{ v(\mathbf{r}, \mathbf{r}_1)$$
$$+ f^{xc}[n_0](\mathbf{r}, \mathbf{r}_1; \omega) \}\, \chi(\mathbf{r}_1, \mathbf{r}_2; \omega)\, v(\mathbf{r}_2, \mathbf{r}'), \qquad (5)$$

which includes all powers in W beyond the G^0W approximation.

A. Bounded electron gas

In the case of a bounded electron gas that is translationally invariant in two directions, such as the jellium surface or the physically motivated model surface described above, the single-particle states entering Eq. (2) are of the form

$$\phi_{\mathbf{k}, i}(\mathbf{r}) = \phi_i(z) e^{i\mathbf{k} \cdot \mathbf{r}_\parallel} \qquad (6)$$

with energies

$$\varepsilon_{\mathbf{k}, i} = \varepsilon_i + k^2/2m_i, \qquad (7)$$

$\mathbf{k}$ being a wave vector parallel to the surface and m_i denoting the effective mass in the plane of the surface.[37]

Introducing Eqs. (6) and (7) into Eq. (1), one finds the following expression for the reciprocal lifetime of a quasiparticle (electron or hole) that has been added in the single-particle state $\phi_{\mathbf{k}, i}(\mathbf{r})$ of energy $\varepsilon_{\mathbf{k}, i}$:

$$\tau_{\mathbf{k}, i}^{-1} = \mp 2 \int dz \int dz'\, \phi_i^*(z) \mathrm{Im}\Sigma(z, z'; \mathbf{k}, \varepsilon_{\mathbf{k}, i}) \phi_i(z'), \quad (8)$$

where $\Sigma(z, z'; \mathbf{k}, \varepsilon_{\mathbf{k}, i})$ represents the two-dimensional (2D) Fourier transform of the self-energy $\Sigma(\mathbf{r}, \mathbf{r}'; \varepsilon_{\mathbf{k}, i})$.

1. G^0W approximation

Using the single-particle wave functions and energies of Eqs. (6) and (7), the G^0W reciprocal lifetime of Eq. (2) yields

$$\tau_{\mathbf{k}, i}^{-1} \ = \ \mp 2 \sum_f \int \frac{d\mathbf{q}}{(2\pi)^2} \int dz \int dz'\, \phi_i^*(z)\, \phi_f^*(z')$$
$$\times \ \mathrm{Im}\, W(z, z'; \mathbf{q}, \omega)\, \phi_i(z')\, \phi_f(z), \qquad (9)$$

where $\omega = |(\varepsilon_i + k^2/2m_i) - (\varepsilon_f + q^2/2m_f)|$, $\mathbf{k}$ and $\mathbf{q}$ represent wave vectors parallel to the surface, and $W(z, z'; \mathbf{k}, \omega)$ denotes the 2D Fourier transform of the screened interaction $W(\mathbf{r}, \mathbf{r}'; \omega)$ of Eq. (3), i.e.,

$$W(z, z'; \mathbf{k}, \omega) \ = \ v(z, z'; \mathbf{k}) + \int dz_1 \int dz_2\, v(z, z_1; \mathbf{k})$$
$$\times \ \chi(z_1, z_2; \mathbf{k}, \omega)\, v(z_2, z'; \mathbf{k}), \qquad (10)$$

$v(z, z'; \mathbf{k})$ and $\chi(z, z'; \mathbf{k}, \omega)$ being 2D Fourier transforms of the bare Coulomb interaction and the density-response function of Eq. (4), respectively.

In the G^0W^0 (or G^0W-RPA) approximation, the reciprocal lifetime is also given by Eqs. (9) and (10), but with the XC kernel $f^{xc}[n_0](\mathbf{r}, \mathbf{r}'; \omega)$ entering Eq. (4) set equal to zero.

2. GWΓ approximation

Using the single-particle wave functions and energies of Eqs. (6) and (7), the $GW\Gamma$ reciprocal lifetime is also found to be given by Eq. (9), but with $W(z, z'; \mathbf{k}, \omega)$ replaced by the 2D Fourier transform of the effective screened interaction $\tilde{W}(\mathbf{r}, \mathbf{r}'; \omega)$ of Eq. (5), i.e.:

$$\tau_{\mathbf{k},i}^{-1} = \mp 2 \sum_f \int \frac{d\mathbf{q}}{(2\pi)^2} \int \mathrm{d}z \int \mathrm{d}z' \, \phi_i^*(z) \, \phi_f^*(z')$$
$$\times \, \mathrm{Im} \, \tilde{W}(z, z'; \mathbf{q}, \omega) \, \phi_i(z') \, \phi_f(z), \qquad (11)$$

where

$$\tilde{W}(z, z'; \mathbf{k}, \omega) = v(z, z'; \mathbf{k}) + \int \mathrm{d}z_1 \int \mathrm{d}z_2 \, \{v(z, z_1; \mathbf{k})$$
$$+ f^{xc}[n_0](z, z_1; \mathbf{k}, \omega)\} \, \chi(z_1, z_2; \mathbf{k}, \omega) \, v(z_2, z'; \mathbf{k}), \quad (12)$$

$f^{xc}[n_0](z, z_1; \mathbf{k}, \omega)$ being the 2D Fourier transform of the XC kernel $f^{xc}[n_0](\mathbf{r}, \mathbf{r}'; \omega)$.

In the $GW^0\Gamma$ approximation, the reciprocal lifetime is also given by Eqs. (11) and (12), thereby with full inclusion of the XC kernel entering Eq. (12), but with the XC kernel entering Eq. (4) set equal to zero.

Hence, we note that both G^0W and $GW\Gamma$ reciprocal lifetimes [Eqs. (9) and (11)] can be calculated from the knowledge of two basic ingredients: (i) single-particle wave functions and energies of the form of Eqs. (6) and (7), which are also basic quantities in the evaluation of the noninteracting density-response function $\chi^0(z, z'; \mathbf{k}, \omega)$, and (ii) the XC kernel $f^{xc}[n_0](z, z'; \mathbf{k}, \omega)$.

B. Single-particle wave functions and energies

For the description of the noninteracting density-response function $\chi^0(z, z'; \mathbf{k}, \omega)$ [and, therefore, the screened interaction $W(z, z'; \mathbf{k}, \omega)$ and the effective screened interaction $\tilde{W}(z, z'; \mathbf{k}, \omega)$ of Eqs. (10) and (12), respectively] single-particle wave functions and energies can safely be taken to be the eigenvalues and eigenfunctions of a *jellium* self-consistent Kohn-Sham hamiltonian.[17] Nevertheless, the actual band structure of *sp* electrons near the surface of noble metals calls for a more realistic description of the single-particle wave functions [$\phi_i(z)$ and $\phi_f(z)$] and energies [ε_i and ε_f] entering Eqs. (9) and (11).

Hence, in the calculations presented in this paper all the single-particle wave functions and energies (those entering Eqs. (9) and (11) and also those involved in the evaluation of the noninteracting density-response function) are taken to be the eigenfunctions and eigenvalues of a physically motivated 1D model hamiltonian that accurately reproduces the projected band gap and the binding energy of the Shockley and the first image state.[33]

C. The XC kernel $f^{xc}[n_0](z, z'; \mathbf{k}, \omega)$

In order to investigate the impact of strong variations of the electron density induced near the surface, and because the excitation energies of interest are typically small (particularly in the case of Shockley holes), we consider the following *adiabatic* ($\omega = 0$) approximations of the XC kernel $f^{xc}[n_0](z, z'; \mathbf{k}, \omega)$:[29]

1. Adiabatic local-density approximation (ALDA)

If one assumes that dynamic electron-density fluctuations are slowly varying in all directions, the XC kernel $f^{xc}[n_0](z, z'; \mathbf{k}, \omega)$ is easily found to be given by the following expression:[38]

$$f^{xc}[n_0](z, z'; \mathbf{k}, \omega) = \bar{f}^{xc}(n_0(z); k^{3D} = 0, \omega = 0) \, \delta(z - z').$$
$$(13)$$

Here, $\bar{f}^{xc}(n_0(z); k^{3D}, \omega)$ is the 3D Fourier transform of the XC kernel of a homogeneous electron gas of density $n_0(z)$, which in the limit as $k^{3D} \to 0$ and $\omega \to 0$ is known to be the second derivative of the XC energy $\varepsilon_{xc}(n)$ per particle of a homogeneous electron gas, to be evaluated at the local density $n_0(z)$. We use the Perdew-Wang parametrization[39] of the difussion Monte Carlo (DMC) XC energy ε_{xc} reported by Ceperley and Alder[40].

2. Refined ALDA

A more accurate description of short-range XC effects can be carried out by replacing the *local* XC kernel $\bar{f}^{xc}(n_0(z); k^{3D} = 0, \omega = 0)$ entering Eq. (13) by a more accurate still adiabatic but momentum-dependent XC kernel $\bar{f}^{xc}(n_0(z), k^{3D} = k, \omega = 0)$ (thus only assuming that the dynamic density fluctuation is slowly varying in the direction perpendicular to the surface), i.e,

$$f^{xc}[n_0](z, z'; \mathbf{k}, \omega) = \bar{f}^{xc}(n_0(z); k^{3D} = k, \omega = 0) \, \delta(z - z').$$
$$(14)$$

Here we exploit the accurate DMC calculations reported by Moroni *et al.*[41] for the static ($\omega = 0$) k^{3D}-dependent *nonlocal* XC kernel $\bar{f}^{xc}$ of a homogeneous electron gas. A parametrization of this data satisfying the well-known small- and large-wavelength asymptotic behaviour was carried out by Corradini *et al.* (CDOP)[42].

3. Adiabatic nonlocal approximation (ANLDA)

Here we still neglect the frequency dependence of the XC kernel (adiabatic approximation), but now we make no assumption on the variation of the dynamic density fluctuation and assume that the *unperturbed* density variation $[n_0(z) - n_0(z')]$ is small within the short range of $f^{xc}[n_0](z, z'; \mathbf{k}, \omega)$. This allows to write

$$f^{xc}[n_0](z, z'; \mathbf{k}, \omega) = \bar{f}^{xc}([n_0(z) + n_0(z')]/2; z, z'; k, \omega = 0), \tag{15}$$

where $\bar{f}^{xc}(n; z, z'; k, \omega)$ represents the 2D Fourier transform of the XC kernel $\bar{f}^{xc}(n; k, \omega)$ of a homogeneous electron gas of density n. An explicit expression for the 2D Fourier transform of the CDOP parametrization of $\bar{f}^{xc}(n; k, \omega = 0)$ was reported in Ref. 29:

$$\bar{f}^{xc}(n; z, z'; k) = -\frac{4\pi e^2 C}{k_F^2}\delta(\tilde{z}) - \frac{2\pi e^2 B}{\sqrt{g k_F^2 + k^2}}e^{-\sqrt{g k_F^2 + k^2}|\tilde{z}|} - \frac{2\alpha\sqrt{\pi/\beta}e^2}{k_F^3}\left[\frac{2\beta - k_F^2\tilde{z}^2}{4\beta^2}k_F^2 + k^2\right]e^{-\beta\left[k_F^2\tilde{z}^2/4\beta^2 + k^2/k_F^2\right]}, \tag{16}$$

where C, B, g, α, and β are dimensionless functions of the electron density (see Ref. 42), $n = k_F^3/3\pi^2$, and $\tilde{z} = z - z'$.

III. RESULTS AND DISCUSSION

On the (111) surface of Cu, the $n = 0$ Shockley state at the center of the surface Brillouin zone ($k = 0$) lies just below the Fermi level, with $\varepsilon_i - \varepsilon_F = -0.445\,\text{eV}$. Binding energies of the $n = 1$ image state on the (111) and (100) surfaces of Cu (measured with respect to the vacuum level) are 0.83 and 0.57 meV, respectively. Effective masses of the $n = 1$ image state on Cu(111) and Cu(100) are close to the free-electron mass ($m_i = 1$),[12] while the effective mass of the $n = 0$ Shockley state on Cu(111) is 0.42.[43,44] The probability density of the $n = 1$ image states on Cu(111) and Cu(100) have a maximum at 2.3 and 3.8 Å, respectively, outside the crystal edge ($z = 0$), which we choose to be located half a lattice spacing beyond the last atomic layer. The $n = 0$ Shockley state wave function in Cu(111), however, is maximum at the crystal edge.

A. Screened interaction

We have carried out calculations of the imaginary part of the screened interaction $W(z, z'; \mathbf{k}, \omega)$ and the effective screened interaction $\tilde{W}(z, z'; \mathbf{k}, \omega)$ of thin slabs. In order to ensure that our slab calculations are a faithful representation of the actual screened interaction of a semiinfinite system, we have used films up to 50 layers of atoms and 80 interlayer-spacing vacuum intervals, as in the G^0W^0 (G^0W-RPA) calculations reported in Refs. 16 and 17.

The impact of XC effects on the imaginary part of the effective screened interaction in the vicinity of the (100) and (111) surfaces of Cu is illustrated in Fig. 2,
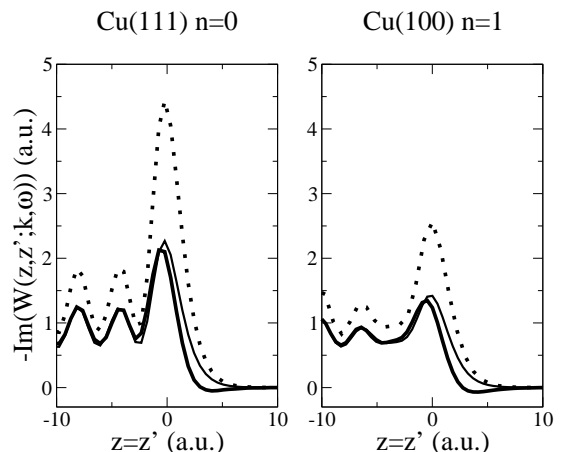

FIG. 2: Imaginary part of the screened interaction $W(z, z'; \mathbf{k}, \omega)$ and the effective screened interaction $\tilde{W}(z, z'; \mathbf{k}, \omega)$, as a function of $z = z'$ and for fixed values of k and ω ($k = 0.5\,\text{Å}^{-1}$ and $\omega = 0.5\,\text{eV}$), in the vicinity of the (100) and (111) surfaces of Cu. ALDA calculations of $\text{Im}\left[\tilde{W}(z, z'; \mathbf{k}, \omega)\right]$ are represented by thick solid lines. RPA and ALDA calculations of $\text{Im}[W(z, z'; \mathbf{k}, \omega)]$ are represented by thin solid and dotted lines, respectively.

where ALDA calculations of $\text{Im}[\tilde{W}(z, z'; \mathbf{k}, \omega)]$ (with full inclusion of XC effects) are compared to calculations of $\text{Im}[W(z, z'; \mathbf{k}, \omega)]$ with (ALDA) and without (RPA) XC effects. Exchange-correlation effects included in the effective screened interaction have two sources, as discussed in Section II A 2. First, there is the reduction of the screening due to the presence of an XC hole associated to all electrons in the Fermi sea [see Eq. (4)], which is included in the calculations represented in Fig. 2 by thick solid lines and *also* in the calculations represented by dotted lines. Secondly, there is the reduction of the effective screened interaction itself due to the XC hole associated to each electron [see Eq. (12)], which is *only* included
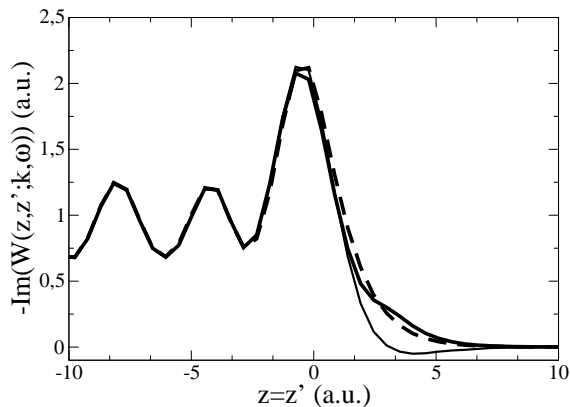
FIG. 3: Imginary part of the effective screened interaction $\tilde{W}(z, z; \mathbf{k}, \omega)$, as a function of $z = z'$ and for fixed values of q and ω ($q = 0.5\,\text{Å}^{-1}$ and $\omega = 0.5\,\text{eV}$), in the vicinity of the (111) surface of Cu. ALDA, refined ALDA, and ANLDA calculations are represented by thin solid, dashed, and thick solid lines, respectively.

FIG. 4: G^0W^0 (G^0W-RPA), G^0W, and $GW\Gamma$ calculations of the imaginary part of the $n = 0$ surface-state self-energy $\Sigma(z, z'; \mathbf{k} = 0, \varepsilon_{\mathbf{k}})$, versus z, in the vicinity of the (111) surface of Cu. The solid circle represents the value of z' in ech case. $GW\Gamma$ calculations (as obtained with the use of our ANLDA XC kernel) are represented by dashed lines. G^0W (also using our ANLDA XC kernel) and G^0W^0 calculations are represented by thin and thick solid lines, respectively. ALDA calculations, which nearly coincide with ANLDA calculations, are not plotted in this figure.

in the calculations represented in Fig. 2 by thick solid lines. These contributions have opposite signs and it is the latter which dominates.

Existing $GW\Gamma$ calculations of the lifetime broadening of image states on Cu(100) and Cu(111) were performed with the ALDA XC kernel that we have used in the calculations represented in Fig. 2. The error introduced by the use of this *local* kernel is small in the interior of the solid, as the wave vectors involved are small ($k < k_F$). However, Fig. 2 shows that the ALDA leads to spurious (negative) results for $\text{Im}[\tilde{W}(z, z'; \mathbf{k}, \omega)]$ near the surface, which is due to the presence of small local values of the Fermi wave vector ($k_F^{local} < k$) in a region where the electron density is small. Hence, we have carried out refined ALDA and adiabatic *nonlocal* (ANLDA) calculations of $\text{Im}[\tilde{W}(z, z'; \mathbf{k}, \omega)]$ (both with full inclusion of XC effects), which have been plotted in Fig. 3. This figure clearly shows that the impact of *nonlocality* on the effective screened interaction is large near the surface, bringing spurious ALDA calculations (thin solid lines) to a more realistic behaviour near the surface (thick solid lines). The refined ALDA scheme partially overcomes the failure of the ALDA, but a full description of the nonlocality of XC effects near the surface might be needed for a realistic description of the absorption power of solid surfaces.

B. Self-energy

Figure 4 exhibits G^0W^0 (G^0W-RPA), G^0W, and $GW\Gamma$ calculations of the imaginary part of the $n = 0$ surface-state self-energy $\Sigma(z, z'; \mathbf{k} = 0, \varepsilon_{\mathbf{k}})$, versus z, in the vicinity of the (111) surface of Cu, with use (in the case of the G^0W and $GW\Gamma$ approximations) of the adiabatic *nonlocal* XC kernel (ANLDA) described in section II C 3. This figure shows that as occurs in the case of the screened
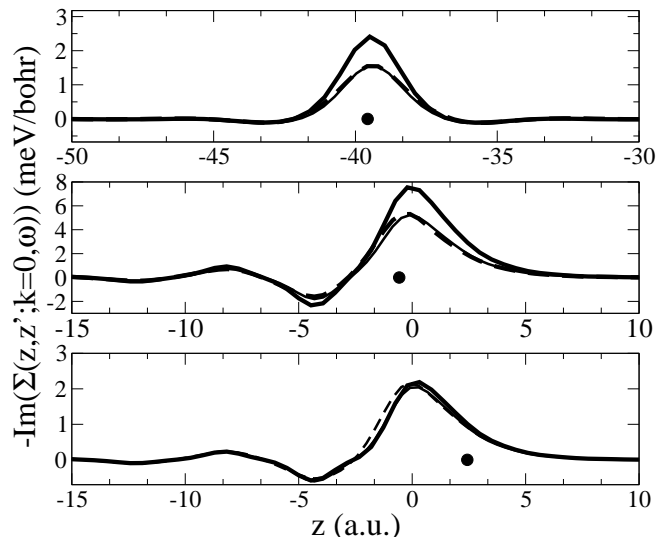
interaction XC effects partially compensate each other, leading to an overall effect of no more than 5%. For comparison, we have also used (in the case of the G^0W and $GW\Gamma$ approximations) the ALDA and refined ALDA kernels described in section II C 3, and we have found that although the use of these local or semilocal kernels leads to spurious results for the screened interaction, our more realistic ANLDA kernel yields self-energies that esentially coincide with those obtained in the ALDA.

C. Reciprocal lifetime

Now we focus on the evaluation of the decay rate (reciprocal lifetime) of surface-state electrons (and holes) at the $n = 1$ (and $n = 0$) surface-state band edge ($\mathbf{k} = 0$) of the (111) and (100) surfaces of Cu. Calculations of the noninteracting density-response function $\chi^0(z, z'; \mathbf{k}, \omega)$ (and, therefore, the reciprocal lifetime) require the introduction of complex frequencies of the form $\omega + i\eta$, η being a positive infinitesimal. Hence, in order to ensure that our numerical calculations yield a converged value of the reciprocal lifetime, we have calculated τ^{-1} as a function of the parameter η. Fig. 5 represents the results we have obtained for the G^0W^0 reciprocal lifetimes of Shockley and image states on the (100) and (111) surfaces of Cu, showing that converged results are obtained for a sufficiently small value of η.

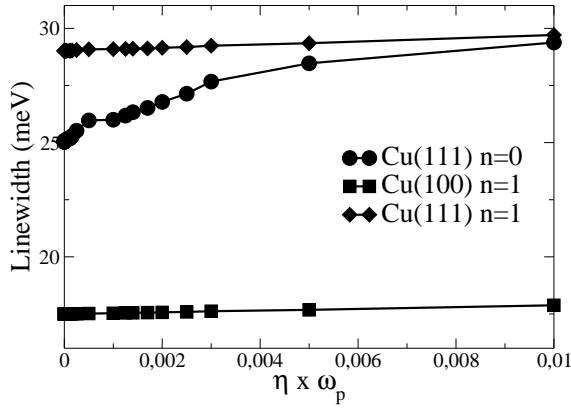Converged calculations of the reciprocal lifetimes of

FIG. 5: G^0W^0 reciprocal lifetimes of Shockley and image states on the (100) and (111) surfaces of Cu, as a function of the parameter η that accounts for the imaginary part of the complex frequencies entering the evaluation of the noninteracting density-response function $\chi^0(z, z'; \mathbf{k}, \omega)$.

TABLE I: G^0W^0, G^0W, and $GW\Gamma$ reciprocal lifetimes, in linewidth units (meV), of an excited surface-state electron (hole) at the $n = 1$ ($n = 0$) surface-state band edge ($\mathbf{k} = 0$) of the (111) and (100) surfaces of Cu. In the case of the G^0W and $GW\Gamma$ reciprocal lifetimes, both ALDA and ANLDA exchange-correlation kernels have been considered.

Surface	n	XC kernel	G^0W^0	G^0W	$GW\Gamma$
Cu(100)	1		17.5		
	1	ALDA		24	17
	1	ANLDA		24.5	17
Cu(111)	0		25		
	0			30	24.5
	0	ANLDA		30.5	24.5
Cu(111)	1		29		
	1	ALDA		42.8	28.5
	1	ANLDA		43	28

Shockley and image states on the (100) and (111) surfaces of Cu are exhibited in Table I. This table shows: (i) G^0W^0 results, which reproduce previous calculations[16,17], (ii) ALDA $GW\Gamma$ results, which in the case of the $n = 1$ image state on Cu(111) and Cu(100) reproduce the calculations reported in Ref. 17 (ALDA $GW\Gamma$ calculations of the reciprocal lifetime of $n = 0$ Shockley states had *not* been reported before), and (iii) ANLDA $GW\Gamma$ calculations, never reported before; for compari-

son, G^0W reciprocal lifetimes are also shown in this table, with use of both the ALDA and the adiabatic *nonlocal* kernel ANLDA described in section II C 3. Differences between our G^0W^0 reciprocal lifetime of the $n = 0$ Shockley state in Cu(111) ($\tau^{-1} = 25\,\text{meV}$) and those reported before[45] ($\tau^{-1} = 19\,\text{meV}$) are simply due to the fact that in our present model we are not accounting for the change of the z-dependent surface-state wave functions $\phi_i(z)$ and $\phi_f(z)$ along the surface-state dispersion curve.

As in the case of the self-energy, the results shown in Table I show that (i) a realistic adiabatic *nonlocal* description of XC effects yields reciprocal lifetimes of Shockley and image states that esentially coincide with those obtained in the ALDA, and (ii) the overall effect of short-range XC is small and $GW\Gamma$ reciprocal lifetimes are close to their G^0W^0 counterparts.

IV. SUMMARY AND CONCLUSIONS

We have carried out extensive calculations of the self-energy and lifetime of Shockley and image states on the (100) and (111) surfaces of Cu, in the framework of the $GW\Gamma$ approximation of many-body theory. This approximation treats on the same footing XC effects between pairs of electrons within the Fermi sea (screening electrons) and between the excited surface-state electron (or hole) and the Fermi sea. We have included XC effects within TDDFT from the knowledge of an adiabatic *nonlocal* XC kernel that goes beyond the local-density approximation, and we have found that these XC contributions (in the screened interaction W and in the expansion of the self-energy in terms of W) have opposite signs and it is the latter which dominates, leading to $GW\Gamma$ reciprocal lifetimes that are only slightly lower than their G^0W^0 counterparts.

[1] J. E. Inglesfield, Rep. Prog. Phys. **45**, 223 (1982).

[2] N. V. Smith, Rep. Prog. Phys. **51**, 1227 (1988).

[3] P. M. Echenique and J. B. Pendry Prog. Surf. Sci. **32**, 111 (1989).

[4] I. E. Tamm, Z. Phys. **76**, 849 (1932).

[5] W. Shockley Phys. Rev. B, **56**, 317 (1939).

[6] P. O. Gartland and B. J. Slagsvold Phys. Rev. B **12**, 4047 (1975).

[7] W. Eberhardt and E.W. Plummer Phys. Rev. B **21**, 3245 (1980).

[8] P.M. Echenique and J.B. Pendry J. Phys. C **11**, 2065 (1978).

[9] V. Dose, Surf. Sci. Rep. **5**, 337 (1985).

[10] S. D. Kevan (Ed.), Angle-resolved Photoemission, vol. 74 of Studies in Surface Science and Catalysis, Elsevier, Amsterdam, 1992.

[11] M. Donath, Surf. Sci. Rep. **20**, 251 (1994).

[12] Th. Fauster and W. Steinmann, in *Photonic Probes of Surfaces*, edited by P. Halevi, Electromagentic Waves: Recent Development in Research Vol. 2 (Elsevier, Amsterdam, 1995).

[13] R. Matzdorf, Surf. Sci. Rep. **20**, 251 (1994).

[14] U. Höfer, I. L. Shumay, Ch. Reuss, U. Thomann, W. Wallauer, and Th. Fauster, Science **277**, 1480 (1997).

[15] A. Eiguren, B. Hellsing, F. Reinert, G. Nicolay, E. V. Chulkov, V. M. Silkin, S. Hüfner, and P. M. Echenique, Phys. Rev. Lett. **88**, 066805 (2002).

[16] E. V. Chulkov, I. Sarria, V. M. Silkin, J. M. Pitarke, and P. M. Echenique, Phys. Rev. Lett. **80**, 4947 (1998).

[17] I. Sarria, J. Osma, E. V. Chulkov, J. M. Pitarke, and P. M. Echenique, Phys. Rev. B **60**, 11795 (1999).

[18] J. Kliewer, R. Berndt, E. V. Chulkov, V. M. Silkin, P. M. Echenique, and S. Crampin, Science, **288**, 1399 (2000).

[19] P.M. Echenique, J. Osma, V.M. Silkin, E.V. Chulkov and J. M. Pitarke, Appl. Phys. A **71**, 503 (2000); P. M. Echenique, J. Osma, M. Machado, V. M. Silkin, E. V. Chulkov, and J. M. Pitarke, Prog. Surf. Sci. **67**, 271 (2000).

[20] A. Fukui, H. Kasai, and A. Okiji, Surf. Sci. **493**, 671 (2001).

[21] P. M. Echenique, R. Berndt, E. V. Chulkov, Th. Fauster, A. Goldmann, and U. Höfer, Surf. Sci. Rep. **52**, 219 (2004).

[22] L. Hedin and S. Lundquist, Solid State Phys. **23**, 1 (1996).

[23] F. Aryasetiawan and O. Gunnarsson, Rep. Prog. Phys. **61**, 237 (1998).

[24] P. M. Echenique, J. M. Pitarke, E. V. Chulkov, and A. Rubio, Chem. Phys. **251**, 1 (2000).

[25] M. Nekovee and J. M. Pitarke, Comput. Phys. Commun. **137**, 123 (2001).

[26] G. D. Mahan and B. E. Sernelius, Phys. Rev. Lett. **62**, 2718 (1989).

[27] G. D. Mahan, *Many Particle Physics* (Plenum, New York, 1990).

[28] I. G. Gurtubay, J. M. Pitarke, and P. M. Echenique, Phys. Rev. B **69**, 245106 (2004).

[29] J. M. Pitarke and J. P. Perdew, Phys. Rev. B. **67**, 045101 (2003).

[30] I. Campillo, J. M. Pitarke, A. Rubio, E. Zarate, and P. M. Echenique, Phys. Rev. Lett. **83**, 2230 (1999); I. Campillo, J. M. Pitarke, A. Rubio, and P. M. Echenique, Phys. Rev. B **62**, 1500(2000).

[31] A. García-Lekue, J. M. Pitarke, E. V. Chulkov, A. Liebsch, and P. M. Echenique, Phys. Rev. Lett. **89**, 096401 (2002); Phys. Rev. B **68**, 045103 (2003).

[32] d electrons do play an important role in the case of image states (but not in the case of Shockley states) on silver surfaces, but this is simply a consequence of the reduction (in the presence of d electrons) of the surface-plasmon energy that allows to open a new decay channel. No surface-plasmon decay channel is opened in the case of the Cu surfaces, since even in the presence of d electrons the Cu surface-plasmon energy is too large for this decay channel to be available.

[33] E. V. Chulkov, V. M. Silkin, and P. M. Echenique, Surf. Sci. **391**, L1217 (1997).

[34] J. M. Pitarke and I. Campillo, Nucl. Instrum. Methods B **164**, 147 (2000); J. M. Pitarke, V. P. Zhukov, R. Keyling, E. V. Chulkov, and P. M. Echenique, ChemPhysChem **5**, 1284 (2004).

[35] E. Runge and E. K. U. Gross, Phys. Rev. Lett. **52**, 997 (1984)

[36] M. Petersilka, U. J. Gossmann, and E. K. U. Gross, Phys. Rev. Lett. **76**, 1212 (1996).

[37] In the case of the jellium surface, the electron motion is free in the plane of the surface and the effective mass coincides, therefore, with that of free electrons. In the case of the model surface, the effective mass is taken from the actual energy dispersion of the projected band structure.

[38] See, e.g., A. Liebsch, *Electronic Excitations at Metal Surfaces* (Plenum Press, New York, 1997).

[39] J. P. Perdew and Y. Wang, Phys. Rev. B **45**, 13244 (1992).

[40] D. M. Ceperley and B. J. Alder, Phys. Rev. Lett. **45**, 566 (1980).

[41] S. Moroni, D. M. Ceperley, and G. Senatore, Phys. Rev. Lett. **75**, 689 (1995).

[42] M. Corradini, R. Del Sole, G. Onida, and M. Palummo, Phys. Rev. B **57**, 14569 (1998).

[43] A. Goldmann, V. Dose, and G. Borstel, Phys. Rev. B **32**, 1971 (1985).

[44] S. L. Hulbert, P. D. Johnson, N. G. Stoffel, W. A. Royer, and N. V. Smith, Phys. Rev. B. **31**, 6815 (1985).

[45] M. G. Vergniory, J. M. Pitarke, and S. Crampin, Phys. Rev. B **72**, 193401 (2005).